HYPOELLIPTIC DIFFUSION AND HUMAN VISION: A SEMI-DISCRETE NEW TWIST ON THE PETITOT THEORY

UGO BOSCAIN, ROMAN CHERTOVSKIH, JEAN-PAUL GAUTHIER, AND ALEXEY REMIZOV

Abstract. This paper is devoted to present an algorithm implementing the theory of neurogeometry of vision, described by Jean Petitot in his book. We propose a new ingredient, namely working on the group of translations and discrete rotations $SE(2,N)$. We focus on the theoretical and numerical aspects of integration of an hypoelliptic diffusion equation on this group. Our main tool is the generalized Fourier transform. We provide a complete numerical algorithm, fully parallellizable. The main objective is the validation of the neurobiological model.

Keywords: neurogeometry, hypoelliptic diffusion, sub-Riemannian geometry, generalized Fourier transform

1. Introduction

In his beautiful book [36], Jean Petitot describes a sub-Riemannian model of the Visual cortex V1.

The main idea goes back to the paper by Hübel an Wiesel in 1959 (Nobel prize in 1981) [27] who showed that in the visual cortex V1, there are groups of neurons that are sensitive to position and directions[1] with connections between them that are activated by the image. The key fact is that the system of connections between neurons, which is called the functional architecture of V1, preferentially connects neurons detecting alignements. This is the so-called *pinwheels* structure of V1.

Therefore it is likely that V1 lifts the images $f(x,y)$ (i.e., functions of two position variables x,y in the plane $\mathbb{R}^2$ of the image) to functions over the projective tangent bundle $PT\mathbb{R}^2$. This bundle has as base $\mathbb{R}^2$ and as fiber over the point (x,y) the set of directions of straight lines lying on the plane and passing through (x,y).

Consider for instance the simplest case in which the image is a smooth curve $\mathbb{R} \ni t \to (x(t),y(t)) \in \mathbb{R}^2$. Lifting this curve to $PT\mathbb{R}^2$ means to add a new variable $\theta(t)$ that is the angle of the vector $(\dot{x}(t),\dot{y}(t))$.

Since we are obliged at some point to go to certain stochastic considerations, it is convenient to write this lift in the following "control form". We say that

Date: January 30, 2013.

2000 *Mathematics Subject Classification.* Primary 93-04; Secondary 93C10, 93C20.

Key words and phrases. Sub-Riemannian geometry, image reconstruction, hypoelliptic diffusion.

[1] Geometers call "directions" (angles modulo π) what neurophysiologists call "orientations".

$(x(\cdot), y(\cdot), \theta(\cdot))$ is the lift of the curve $(x(\cdot), y(\cdot))$ if there exist two functions $u(\cdot)$ and $v(\cdot)$ (called controls) such that[2]

$$\begin{pmatrix} \dot{x}(t) \\ \dot{y}(t) \\ \dot{\theta}(t) \end{pmatrix} = u(t) \begin{pmatrix} \cos(\theta(t)) \\ \sin(\theta(t)) \\ 0 \end{pmatrix} + v(t) \begin{pmatrix} 0 \\ 0 \\ 1 \end{pmatrix}. \tag{1.1}$$

Here the control $u(t)$ plays the role of the modulus of the planar vector $(\dot{x}(t), \dot{y}(t))$, but can take positive and negative values since the angle $\theta(t)$ is defined modulo π. The control $v(t)$ is just the derivative of $\theta(t)$.

Remark 1. *The vector distribution* $\blacktriangle(x, y, \theta) := \operatorname{span}\{F(x, y, \theta), G(x, y, \theta)\}$, *where*[3]

$$F(x, y, \theta) = \begin{pmatrix} \cos(\theta) \\ \sin(\theta) \\ 0 \end{pmatrix}, \; G(x, y, \theta) = \begin{pmatrix} 0 \\ 0 \\ 1 \end{pmatrix},$$

endows $PT\mathbb{R}^2$ *with the structure of a contact manifold. Indeed* $\blacktriangle$ *is completely non-integrable (in the Frobenius sense) since* F *and* G *satisfy the Hörmander condition:* $\operatorname{span}\{F, G, [F, G]\} = T_q PT\mathbb{R}^2$ *for each* $q \in PT\mathbb{R}^2$.

In the model described by Petitot, when a curve is partially interrupted, it is reconstructed by minimizing the energy necessary to activate the regions of the visual cortex that are not excited by the image. Roughly speaking, neurons of V1 are grouped into orientation columns, each of them being sensitive to visual stimuli at a given point of the retina and for a given direction on it. Orientation columns are themselves grouped into hypercolumns, each of them being sensitive to stimuli at a given point with any direction (see Figure 1).

In the visual cortex there are two types of connections: the *vertical* connections among orientation columns in the same hypercolumn, and the *horizontal* connections among orientation columns belonging to different hypercolumns and sensitive to the same orientation. For an orientation column it is easy to activate another orientation column which is a "first neighbor" either by horizontal or by vertical connections.

In the model described by Petitot the energy necessary to activate a path $[0, T] \ni t \mapsto (x(t), y(t), \theta(t))$ is given by

$$\int_0^T \left(\dot{x}(t)^2 + \dot{y}(t)^2 + \frac{1}{\alpha} \dot{\theta}(t)^2 \right) dt = \int_0^T \left(u(t)^2 + \frac{1}{\alpha} v(t)^2 \right) dt.$$

The term $\dot{x}(t)^2 + \dot{y}(t)^2$ is proportional to the energy necessary to activate horizontal connections, while the term $\dot{\theta}(t)^2$ is proportional to the energy necessary to activate vertical connections. The parameter $\alpha > 0$ is a relative weight.

---

[2] Which curves can be lifted with this procedure is an interesting question (see for instance [9]). In this paper we are not focused on this problem. Let us just observe that a planar curve having a cusp (as for instance $[-1, 1] \ni t \mapsto (t^3, t^2)$) has a smooth lift.

[3] Notice that the definition of vector field F is not global over $PT\mathbb{R}^2$ since it is not continuous at $\theta = \pi \sim 0$: the distribution $\blacktriangle$ is not trivializable and a correct definition of it would require two charts. However, for sake of simplicity, we proceed with a single chart with some abuse of notation. Notice, however, that if we lift the problem to the group $SE(2)$, which is a double covering of $PT\mathbb{R}^2$, the structure becomes trivializable and the definition of F becomes global. We do this often along the paper.

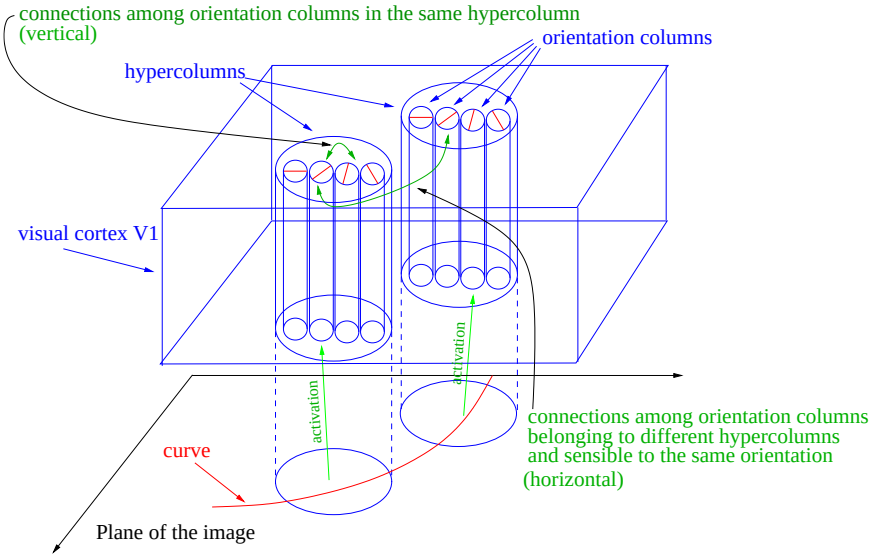

FIGURE 1. The structure of V1

To conclude, in V1, the problem of reconstructing a curve interrupted between the boundary conditions (x_0, y_0, θ_0) and (x_1, y_1, θ_1) becomes the optimal control problem[4]

$$\begin{pmatrix} \dot{x}(t) \\ \dot{y}(t) \\ \dot{\theta}(t) \end{pmatrix} = uF(x,y,\theta) + vG(x,y,\theta),$$

$$\int_0^T \left(u(t)^2 + \frac{1}{\alpha} v(t)^2 \right) dt \to \min,$$

$$(x(0), y(0), \theta(0)) = (x_0, y_0, \theta_0), \ (x(T), y(T), \theta(T)) = (x_1, y_1, \theta_1). \tag{1.2}$$

Finding the solution to this optimal control problem can be seen as the problem of finding the minimizing geodesic for the sub-Riemannian structure over $PT\mathbb{R}^2$ defined as follows: The distribution is $\blacktriangle$ and the metric g_α over $\blacktriangle$ is the one obtained by claiming that the vector fields F and $\sqrt{\alpha}\, G$ form an orthonormal frame. By construction, this sub-Riemannian manifold is invariant under the action of the group of rototranslations of the plane $SE(2)$. Indeed, $\{\blacktriangle, g_\alpha\}_{\alpha \in]0,\infty[}$ are all the sub-Riemannian structures over $PT\mathbb{R}^2$ which are invariant under the action of $SE(2)$. See for instance [2].

Remark 2. *From the theoretical point of view, the weight parameter α is irrelevant: for any $\alpha > 0$ there exists a homothety of the (x, y)-plane that maps geodesics of the metric with the weight parameter α to those of the metric with $\alpha = 1$. For this reason, in all theoretical considerations we fix $\alpha = 1$. However its role will be important in our inpaiting algorithms (see Section 2.3).*

[4] Here the time T should be fixed, but changing T changes only the parameterization of the solutions. For the same reasons as in Riemannian geometry, minimizer of the sub-Riemannian energy $\int_0^T \left(u(t)^2 + \frac{1}{\alpha} v(t)^2 \right) dt$ are minimizers of the sub-Riemannian length $\int_0^T \sqrt{u(t)^2 + \frac{1}{\alpha} v(t)^2}\, dt$.

The history of this model goes back to the paper by Hoffman [25] in 1989, who first proposed to regard the visual cortex as a manifold with a contact structure. In 1998, Petitot [34, 35] wrote the first version of the sub-Riemannian problem on the Heisenberg group and gave an enormous impulse to the research on the subject. In 2006, Citti and Sarti [13] required the invariance under rototranslations and wrote the model on $SE(2)$. In [8], it was proposed to write the problems on $PT\mathbb{R}^2$ to avoid some topological problems and to be more consistent with the fact that the visual cortex V1 is sensitive only to directions (i.e., angles modulo π) and not to directions with orientations (i.e., angles modulo 2π). The theory was wonderfully completed in Petitot's book [36]. It should be also mentioned that many crucial suggestions were made by A. Agrachev.

The detailed study of geodesics was performed by Yuri Sachkov in a series of papers [37, 38]. For modifications of the model aimed to avoid the presence of geodesics whose projection on the plane has cusps, see [13, 39, 7, 9]. This model was also deeply studied by Duits et al. in [16, 17, 18] with medical imaging applications in mind, and by Hladky and Pauls [24]. Of course this model has some close relations with the celebrated model by Mumford [32].

The model described by Petitot was used to reconstruct smooth images by Ardentov, Mashtakov and Sachkov [6]. The technique developed by them consists of reconstructing as minimizing geodesics the level sets of the image where they are interrupted. Obviously, when applying this method to reconstruct images with large corrupted parts, one is faced to the problem that it is not clear how to put in correspondence the non-corrupted parts of the same level set.

For that reason, to reconstruct a corrupted image (the V1 inpainting problem), it is natural to proceed as follows: in system (1.1), excite all possible admissible paths in a stochastic way. One gets a stochastic differential equation

$$\begin{pmatrix} dx_t \\ dy_t \\ d\theta_t \end{pmatrix} = \begin{pmatrix} \cos(\theta_t) \\ \sin(\theta_t) \\ 0 \end{pmatrix} du_t + \begin{pmatrix} 0 \\ 0 \\ 1 \end{pmatrix} dv_t, \tag{1.3}$$

where u_t, v_t are two independent Wiener processes.

Consider the associated diffusion process (here we have fixed $\alpha = 1$):

$$\frac{\partial \psi}{\partial t} = \frac{1}{2}\Delta\psi, \quad \Delta = F^2 + G^2 = \left(\cos(\theta)\frac{\partial}{\partial x} + \sin(\theta)\frac{\partial}{\partial y}\right)^2 + \frac{\partial^2}{\partial \theta^2}. \tag{1.4}$$

The operator Δ is not elliptic, but it is hypoelliptic (satisfies Hörmander condition). By the Feynman–Kac formula, integrating Equation (1.4) with the corrupted image as the initial condition, **one expects to reconstruct the most probable missing level curves** (among admissible).

To summarize, in this model, the process of reconstruction by V1 of corrupted images is the following

- The plane image $f(x, y)$ is lifted to a certain "function" $\overline{f}(x, y, \theta)$ on the bundle $PT\mathbb{R}^2$.
- The diffusion process (1.4) with the initial condition $\psi\big|_{t=0} = \overline{f}$ is integrated on the interval $t \in [0, T]$ for some $T > 0$.
- The resulting function $\overline{f}_T = \psi\big|_{t=T}$ on the bundle $PT\mathbb{R}^2$ is projected down to a function $f_T(x, y)$, which represents the reconstructed image.

The lifting procedure should be as follows: the image is assumed to be a smooth[5] function $f(x, y)$. Then, it can be naturally lifted to a surface S in $PT\mathbb{R}^2$ by lifting its level curves. At a point (x, y, θ) we would like to set $\overline{f}(x, y, \theta) = f(x, y)$ if $(x, y, \theta) \in S$ and $\overline{f}(x, y, \theta) = 0$ elsewhere. But this would be nonsense since S has zero measure in $PT\mathbb{R}^2$. Hence, $f(x, y)$ is lifted to a distribution $\overline{f}(x, y, \theta)$, supported in S, and weighted by $f(x, y)$. We refer to [8] for details.

The idea of modeling the process of reconstruction of images in V1 as an hypoelliptic diffusion was presented first in [13] and was implemented in details with some slight modifications and different purposes in [39, 8, 17, 18]. A clever variant to the lifting process was proposed in [17, 18].

It turns out that although looking rather simple, Equation (1.4) is not that easy to integrate numerically. In particular, the multiscale sub-Riemannian effects are hidden inside. (The numerical literature for PDEs in sub-Riemannian geometry appears to be very scarce.)

For the equation (1.4) it is possible to compute the associated heat kernel, see [3] and [16, 17]; however, the direct use of the kernel quickly appears to be not very tractable. Moreover, the numerical integration starts to be a rather large problem, due to the number of points/angles in a reasonable image. To get an idea of the size of the full space-discretization of the problem, see Remark 5 below.

For these reasons, only very recently, some promising results about inpainting using hypoelliptic diffusion were obtained in [8]. In that paper a sophisticated algorithm based upon the generalized Fourier transform on the group SE(2) was used.

In this paper, we introduce a new ingredient, namely we conjecture the following:

- the visual cortex can detect a finite (small) number of directions only.

This conjecture is based on the observation of the organization of the visual cortex in pinwheels. The planar and the angular degrees of freedom cannot be treated in the same way. We conjecture that there are topological constraints that prevent the possibility of detecting a continuum of directions even when sending the distance between pinwheels to zero.

In this paper we are not going to justify this conjecture. Rather, we concentrate on the effect of this conjecture on the mathematical model and on our ability to integrate the hypoelliptic diffusion equation.

The main purpose of this paper is to write an inpainting algorithm which makes use of the group of continuous translations and discrete rotation $SE(2, N)$. This group has very special features: it is maximally almost periodic, and all its unitary irreducible representations are finite dimensional. Moreover, for this group the heat kernel can be written in a very simple form (see Sections 2.2.2 and 2.2.3).

In the following, when using the group $SE(2, N)$ instead than $SE(2)$ for inpaiting, we speak of the "semi-discrete variant" to the Petitot theory.

It turns out that we were led to rather abstract considerations, to get at the end a quite simple algorithm, massively parallelizable. This aspect of parallelizability seems to fit with the structure of the visual cortex V1, which is thought to make a lot of parallel computations.

[5] In fact, it is known by biologists that a certain smoothing procedure is already applied at the level of the retina [15, 30, 33].

The paper is organized as follows: in the next section 2, we discuss some properties of the group $SE(2)$ and its discrete avatars, together with a discrete version of the hypoelliptic diffusion (1.4).

Section 3 presents our main ideas and shows a first algorithm, which is not suitable in our case, mostly for two reasons:

- The "distributional" nature of lifted images (initial conditions).
- Compared to our final algorithm, it does not present the same capability to treat in a different way the corrupted and non-corrupted parts of the image (see Section 5).

However, this approach could certainly be interesting for more smooth initial conditions.

Section 4 presents our final algorithm that, due to the abstract structure of the groups under consideration, is massively parallel: It reduces the problem to a number of problems of integration of linear differential equations in low dimension, completely decoupled.

Section 5 presents some heuristic improvements of the algorithm in the case where we can distinguish between the corrupted and non-corrupted parts of the image.

In Appendix A, we present a series of results of reconstruction with high corruption rates and the table of all parameters used for the reconstruction procedures. These parameters include: the time of diffusion, the weight α, and other parameters that are used to "tune" the action of the diffusion on the corrupted and non corrupted points.

Finally, Appendix B is devoted to basic theoretical concepts and to certain technical computations.

We do not pretend that our results are better than the inpainting algorithms existing today. We just claim that they really seem to validate the theory described by Jean Petitot and our semi-discrete variant. Moreover we emphasize the global character of the basic algorithm.

We do not discuss the final step of the algorithm (projection) here. There are at least two obvious possibilities: projecting by taking either the maximum, or the average, over angles. Numerous experiments show that the projection made by the maximum provides better results.

2. The Operators and the groups under consideration

2.1. **Groups.** We advise the uninitiated reader to start with our paper [3] and to have a look to Appendix B at the end of this paper.

2.1.1. *The group of Motions SE(2).* The group law over the Lie group $SE(2)$ has multiplication law $(X_2, \theta_2) \cdot (X_1, \theta_1) = (X_2 + R_{\theta_2} X_1, \theta_1 + \theta_2)$, where

$$X = \begin{pmatrix} x \\ y \end{pmatrix}, \quad R_\theta = \begin{pmatrix} \cos(\theta) & \sin(\theta) \\ -\sin(\theta) & \cos(\theta) \end{pmatrix},$$

R_θ is the rotation of angle θ in the X-plane.

The (strongly continuous) unitary irreducible representations of $SE(2)$ are well known. However for analogy with the next section, we need to recall basic facts. For a survey, see [40, 41].

As representations of a semi-direct product, they can be obtained by using Mackey's imprimitivity theorem, and therefore, they are parametrized by the orbits of the (contragredient) action of rotations on the X-plane, i.e., they are parametrized by the half lines passing through the origin. Additionally, corresponding to the origin, there are the characters of the rotation group S^1 that do not count in the support of the Plancherel's measure. Finally, the representation χ_λ corresponding to the circle of radius λ acts over $L^2(S^1)$, and is given by

$$[\chi_\lambda(X,\theta)\cdot\varphi](u) = e^{i\langle v_\lambda, R_u X\rangle}\varphi(u+\theta),$$

where v_λ is a vector of length λ in $\mathbb{R}^2$ and $\langle\cdot,\cdot\rangle$ denotes the standard Euclidean scalar product over $\mathbb{R}^2$.

Note that $SE(2)$ is far from being maximally almost periodic, since all its finite dimensional unitary irreducible representations are given by the characters of S^1 only.

Let us also recall [3, 8, 16, 17] that the sub-Riemannian heat kernel on $SE(2)$, corresponding to the hypoelliptic Laplacian $\frac{1}{2}\Delta$ defined in (1.4) is given by[6]

$$P_t(X,\theta) = \frac{1}{2}\int_0^{+\infty}\Bigg(\sum_{n=0}^{+\infty} e^{a_n^\lambda t}\left\langle \mathrm{ce}_n\left(\theta,\frac{\lambda^2}{4}\right),\, \chi_\lambda(X,\theta)\,\mathrm{ce}_n\left(\theta,\frac{\lambda^2}{4}\right)\right\rangle + \sum_{n=0}^{+\infty} e^{b_n^\lambda t}\left\langle \mathrm{se}_n\left(\theta,\frac{\lambda^2}{4}\right),\, \chi_\lambda(X,\theta)\,\mathrm{se}_n\left(\theta,\frac{\lambda^2}{4}\right)\right\rangle \lambda d\lambda, \tag{2.1}$$

where the functions se_n and ce_n are the 2π-periodic Mathieu sines and cosines, and $a_n^\lambda = -\frac{\lambda^2}{4} - a_n\big(\frac{\lambda^2}{4}\big)$, $b_n^\lambda = -\frac{\lambda^2}{4} - b_n\big(\frac{\lambda^2}{4}\big)$, with a_n, b_n, the characteristic values for the Mathieu equation.

Then the solution of the diffusion equation (1.4) with the initial condition $\psi\big|_{t=0}=\psi_0$ is given by the right-convolution formula:

$$\psi(t,X,\theta) = e^{t\Delta}\psi_0(X,\theta) = \psi_0(X,\theta) * P_t(X,\theta) = \int_{SE(2)} \psi_0(g) P_t\big(g^{-1}\cdot(X,\theta)\big)\, dg, \tag{2.2}$$

where $g\in SE(2)$ and dg is the Haar measure: $dg = dxdyd\theta$. Unfortunately, in practice formula (2.2) is not very tractable, for several reasons (in particular, due to the slow convergence and the difficulty to find good computer implementations of Mathieu functions).

2.1.2. *The group of discrete motions $SE(2,N)$.* In the next section, a discrete-angle version of the above diffusion equation will appear naturally. It corresponds to the group of motions $SE(2)$ restricted to rotations with angles $\frac{2k\pi}{N}$. This group is denoted by $SE(2,N)$. It has very special features: it is maximally almost periodic, and all its unitary irreducible representations are finite dimensional (it is a Moore group, see [23] for details), although it is not compact. This follows in particular from [19, 16.5.3, page 304]: it is the semi-direct product of a compact subgroup $K = \mathbb{Z}/N\mathbb{Z}$, and a normal subgroup V isomorphic to $\mathbb{R}^2$, each element of V commuting with the connected component of the identity (which in this case is V itself). To simplify, we set $R_k = R_{\frac{2k\pi}{N}}$.

[6] in this formula $\alpha = 1$

Besides the characters of K, the representations coming in the support of the Plancherel measure are parametrized by $(\lambda,\nu)\in\mathbb{R}^+_*\times[0,\frac{2\pi}{N}[=\widehat{SE(2,N)}$, the **dual**[7] of $SE(2,N)$. They act on $\mathbb{C}^N$ and are given by

$$\chi_{\lambda,\nu}(X,r)=\mathrm{diag}_k\big(e^{i\langle V_{\lambda,\nu},R_kX\rangle}\big)S^r, \tag{2.3}$$

where $\mathrm{diag}_k\big(e^{i\langle V_{\lambda,\nu},R_kX\rangle}\big)$ is the diagonal matrix with diagonal elements $e^{i\langle V_{\lambda,\nu},R_kX\rangle}$, $V_{\lambda,\nu}=(\lambda\cos(\nu),\lambda\sin(\nu))$, $k=1,\dots,N$, and S is the shift matrix over $\mathbb{C}^N$ (i.e., $Se_k=e_{k+1}$ for $k=1,\dots,N-1$, and $Se_N=e_1$).

2.2. **The semi-discrete diffusion operator.**

2.2.1. *Semi-discrete versus continuous.* Firstly, we show that a certain semi-discrete (discretization with respect to the angle) model of the diffusion is compatible with the limit continuous model. For the considerations in this section, one may refer to the paper [5].

The diffusion equation (1.4) comes from the stochastic differential equation (1.3), where u_t, v_t are two independent standard Wiener processes. It is the associated Fokker-Planck (or Kolmogorov forward) equation to (1.3).

From the image processing point of view, integrating the diffusion is equivalent to excite all possible admissible paths, in a stochastic way.

In fact, in the real structure of the V1 cortex, **a finite (small) number of angles only is taken into account**. Here this number is denoted by N.

Therefore, it is natural to consider the following stochastic process with jumps evidently connected with the stochastic equation (1.3):

$$dz_t=\begin{pmatrix}dx_t\\dy_t\end{pmatrix}=\begin{pmatrix}\cos(\theta_t)\\\sin(\theta_t)\end{pmatrix}dv_t, \tag{2.4}$$

in which θ_t is a jump process. Set $\Lambda_N=(\lambda_{i,j})$, $i,j=0,\dots,N-1$, where

$$\lambda_{i,j}=\lim_{t\to0}\frac{\mathsf{P}\,[\theta_t=e_j|\theta_0=e_i]}{t}\quad\text{for}\quad i\neq j,\quad \lambda_{j,j}=-\sum_{i\neq j}\lambda_{i,j}.$$

The matrix Λ_N is the infinitesimal generator of the jump process.

We assume Markov processes, where the law of the first jump time is exponential, with parameter $\beta>0$ (that will be specified later on). The jump has probability $\frac12$ on both sides. Then we get a Poisson process, and the probability of k jumps between 0 and t is

$$\mathsf{P}\,[k\text{ jumps}]=\frac{(\beta t)^k}{k!}e^{-\beta t}.$$

So that:

$$\begin{aligned}
\mathsf{P}\,[\theta_t=e_{i\pm1}|\theta_0=e_i]&=\frac12\big(\beta t+kt^2+o(t^2)\big)e^{-\beta t},\\
\mathsf{P}\,[\theta_t=e_{i\pm2}|\theta_0=e_i]&=\frac14\left(\frac12\beta^2t^2+o(t^2)\right)e^{-\beta t},\\
\mathsf{P}\,[\theta_t=e_{i\pm n}|\theta_0=e_i]&=O(t^n)e^{-\beta t},\quad n=2,3,\dots,
\end{aligned}$$

with the convention that e_i is modulo N.

[7] The natural "dual topology" of $\widehat{SE(2,N)}$ is that of a cone, that consists of considering $\mathbb{R}^+_*\times[0,\frac{2\pi}{N}]$ and identifying $(\lambda,0)$ with $(\lambda,\frac{2\pi}{N})$.

Hence $\lambda_{i,i\pm1} = \frac{1}{2}\beta$ and $\lambda_{i,i} = -\beta$. All other elements of the matrix Λ_N are equal to zero. Then, the infinitesimal generator of the semi-group associated with the stochastic process (z_t, θ_t) is of the form:

$$\mathcal{L}_N\Psi(z, e_i) = (A\Psi)_i(z) + (\Lambda_N\Psi(z, e_i))_i, \tag{2.5}$$

where $\Psi_j(z) = \Psi(z, e_j)$, $z = (x, y)$, and

$$(A\Psi)_i(z) = A\Psi(z, e_i) = \frac{1}{2}\left(\cos(e_i)\frac{\partial}{\partial x} + \sin(e_i)\frac{\partial}{\partial y}\right)^2 \Psi(z, e_i), \tag{2.6}$$

$$(\Lambda_N\Psi(z, e_i))_i = \sum_{j=0}^{n-1} \lambda_{i,j}\Psi_j(z) = \frac{\beta}{2}\big(\Psi_{i-1}(z) - 2\Psi_i(z) + \Psi_{i+1}(z)\big), \tag{2.7}$$

where the subscript i means the i-th coordinate of the vector.

Therefore, if we set $\beta = \left(\frac{N}{2\pi}\right)^2$, we get

$$(\Lambda_N\Psi(z, e_i))_i = \frac{1}{2}\frac{\Psi_{i-1}(z) - 2\Psi_i(z) + \Psi_{i+1}(z)}{\left(\frac{2\pi}{N}\right)^2} = \frac{1}{2}\frac{\partial^2}{\partial\theta^2}\Psi(z, e_i) + O\Big(\frac{1}{N}\Big)^2.$$

At the limit $N \to \infty$, from formulae (2.5) – (2.7) we get the second order differential operator

$$\mathcal{L}\Psi(z, \theta) = \frac{1}{2}\left(\left(\cos(\theta)\frac{\partial}{\partial x} + \sin(\theta)\frac{\partial}{\partial y}\right)^2 + \frac{\partial^2}{\partial\theta^2}\right)\Psi(z, \theta) = \frac{1}{2}\Delta\Psi(z, \theta),$$

that is, the operator of our diffusion process (1.4). However the exact Fokker-Planck equation[8] with number of angles $N \ll \infty$ contains the parameter β:

$$\begin{aligned}\frac{d\psi_r}{dt}(t, z) = \frac{1}{2}\left(\cos(e_r)\frac{\partial}{\partial x} + \sin(e_r)\frac{\partial}{\partial y}\right)^2 \psi_r(t, z) + \\ \frac{\beta}{2}\big(\psi_{r-1}(t, z) - 2\psi_r(t, z) + \psi_{r+1}(t, z)\big), \quad r = 0, \dots, N-1.\end{aligned} \tag{2.8}$$

2.2.2. *The semi-discrete heat kernel via the GFT.* The GFT (generalized non-commutative Fourier transform, see [3] and Appendix B) transforms our hypoelliptic diffusion equation into a continuous sum of diffusions with elliptic right-hand term, and the summation over $\widehat{SE(2, N)}$ is with respect to the Plancherel measure $\lambda d\lambda d\nu$. We compute the semi-discrete heat kernel via the GFT, just as in [3], and we get a similar but simpler formula than for the "continuous" heat kernel (2.1) in the case of the group $SE(2)$:

Formulae (B.1) and (B.2) for the direct and the inverse GFT show that, if we set

$$\widetilde{A}_{\lambda,\nu} = \Lambda_N - \mathrm{diag}_k\big(\lambda^2\cos^2(e_k - \nu)\big), \tag{2.9}$$

we get the following expression for the "semi-discrete" (or "jump") heat kernel:

$$D_t(z, e_r) = \int\limits_{\widehat{SE(2,N)}} \mathrm{trace}\Big(e^{\widetilde{A}_{\lambda,\nu}t} \cdot \mathrm{diag}_k\Big(e^{i\langle V_{\lambda,\nu}, R_k z\rangle}\Big)S^r\Big)\lambda d\lambda d\nu. \tag{2.10}$$

[8]Note that here, due to self adjointness, the Kolmogorov-backward equation is the same as the Kolmogorov-forward one (Fokker-Planck).

Note also that it is a closed formula similar to the one in the Heisenberg case (explicit usual functions modulo a Fourier transform). These are the only cases we know for noncompact groups, where the kernel is obtained with such an explicit formula.

2.2.3. *A direct way to compute the semi-discrete heat kernel.* We start from our semi-discrete heat equation (2.8). The heat kernel is the convolution kernel associated with $D_t(z, e_r)$, the fundamental solution of Equation (2.8).

Applying the ordinary Fourier Transform with respect to the space variable z to (2.8), we get the ordinary linear differential equation

$$\frac{d}{dt}\widetilde{D}_t(z) = \widetilde{A}_{\lambda,\nu}\widetilde{D}_t(z), \tag{2.11}$$

where $\widetilde{D}_t(z) = \big(D_t(z, e_1), \dots, D_t(z, e_N)\big)$, with the initial condition obtained from the Dirac delta function at the identity by the ordinary Fourier Transform:

$$\widetilde{D}_0(z) = \delta_N = (0, \dots, 0, 1).$$

Then, taking the inverse ordinary Fourier Transform with respect to the space variable, we get a second expression for the heat kernel:

$$D_t(z, e_r) = \int_{\mathbb{R}^2} \Big(e^{\widetilde{A}_{\lambda,\nu}t}\delta_N\Big)_r e^{i\langle V_{\lambda,\nu}, z\rangle}\lambda d\lambda d\nu. \tag{2.12}$$

Remark 3. *Looking at the formulae* (2.10) *and* (2.12)*, it is not clear that these expressions are identical. The proof of this fact is given in Appendix B.3. Although less direct, we prefer formula* (2.10)*, that reflects more the structure of* $SE(2, N)$*.*

2.3. **The weighting of the metric.** Consider the diffusion process

$$\frac{\partial\psi}{\partial t} = \frac{1}{2}\Delta_\alpha\psi, \quad \Delta_\alpha = F^2 + \alpha G^2 = \left(\cos(\theta)\frac{\partial}{\partial x} + \sin(\theta)\frac{\partial}{\partial y}\right)^2 + \alpha\frac{\partial^2}{\partial\theta^2} \tag{2.13}$$

with the weighting coefficient $\alpha > 0$. The hypoelliptic operator Δ defined in (1.4) is the case $\alpha = 1$. Although the coefficient α is theoretically irrelevant (see Remark 2), it plays an essential role in practice.

On the same way, for the semi-discrete operator, we have

$$\begin{aligned}
&\Delta^{(N)}\psi_i(t, z) = \\
&\left(\cos(e_i)\frac{\partial}{\partial x} + \sin(e_i)\frac{\partial}{\partial y}\right)^2 \psi_i(t, z) + \beta\big(\psi_{i-1}(t, z) - 2\psi_i(t, z) + \psi_{i+1}(t, z)\big) = \\
&\qquad\qquad \left(\left(\cos(e_i)\frac{\partial}{\partial x} + \sin(e_i)\frac{\partial}{\partial y}\right)^2 + \beta\Big(\frac{2\pi}{N}\Big)^2\frac{\partial^2}{\partial\theta^2}\right)\psi_i(t, z) + O\Big(\frac{1}{N}\Big)^2
\end{aligned}$$

as $N \to \infty$. Comparing the above formula with (2.8), we have the relation:

$$\alpha = \beta\Big(\frac{2\pi}{N}\Big)^2. \tag{2.14}$$

It appeared clearly in all our experiments that $N = 30$ is always enough (it brings nothing visible in the experiments to take $N > 30$).

Both parameters N and β have a physiological meaning. Therefore, the coefficient α of the limit behavior ($N \to \infty$) can certainly be obtained from physiological considerations.

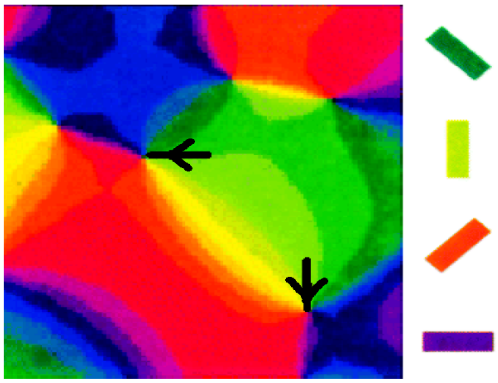

FIGURE 2. Two pinwheels with opposite chirality. Each color corresponds to the sensitivity to one direction.

2.4. **The effect of the projectivisation on the kernel.** The orientation maps of the V1 cortex show "pinwheels", that is, singularities where iso-direction lines of any orientation θ converge. Pinwheels have "chirality", that is, they rotate as 2θ or -2θ along a small direct loop around them. This could be reflected in formula (2.15) below. See Figure 2.

As we said, the neurons are not sensitive to the angles themselves, but to directions only (i.e., the angles are modulo π and not 2π). It is the reason why we work in the projectivisation $PT\mathbb{R}^2$ of the tangent bundle of $\mathbb{R}^2$, in place of $SE(2)$ itself. From the discrete point of view, it means that if N is the number of values of directions (not angles), the angle-step is in fact $\frac{\pi}{N}$.

Also, as it was explained in [8], the sub-Riemannian structure over $PT\mathbb{R}^2$ itself is not trivializable. This is not a problem for the operators Δ and $\Delta^{(N)}$, since the functions $\cos(\theta)^2$, $\sin(\theta)^2$ and $\sin(2\theta)$ are π-periodic. **Hence, details relative to this projectivisation are omitted in the following sections**.

From the point of view of the heat kernels, in fact, if p_t denotes the heat kernel over $PT\mathbb{R}^2$ (which is not a group convolution kernel anymore, since $PT\mathbb{R}^2$ is not a group), we have the formula

$$p_t((x,y,\theta),(\bar{x},\bar{y},\bar{\theta})) = P_t((\bar{x},\bar{y},\bar{\theta})^{-1}\cdot(x,y,\theta)) + P_t((\bar{x},\bar{y},\bar{\theta})^{-1}\cdot(x,y,\theta+\pi)), \tag{2.15}$$

where the inverses and products are intended in the group $SE(2)$.

A similar formula holds for the semi-discrete kernels d_t and D_t (from (2.10)) for even N.

3. A PRE-ALGORITHM

As we said in section 2.1.2, the group $SE(2,N)$ is maximally almost periodic. It follows from the expression (2.3) of the unitary irreducible representations that the Bohr-almost periodic functions $f(x,y,r)$ are just those such that the functions $f_r(x,y) = f(x,y,r)$, $r = 1,\dots,N$, are Bohr-almost periodic over $\mathbb{R}^2$ in the usual sense. We call $AP(N)$ the set of almost periodic functions on $SE(2,N)$, and we identify the elements of $AP(N)$ to $\mathbb{C}^N$-valued functions whose components are almost periodic over $\mathbb{R}^2$, i.e., functions that are uniform limits of trigonometric polynomials in the two variables (x,y).

These functions are dense among continuous functions over any compact subset of $SE(2,N)$, and $AP(N)$ is a good candidate for the space of solutions of our heat equation: exactly as for the usual heat equation (see [14, pp. 144–146] for instance), the uniformly bounded solutions of our heat equation with initial conditions in $AP(N)$ remain almost periodic over $SE(2,N)$ uniformly in time.

Functions coming from practical images have support in a bounded subset of $SE(2,N)$. They can be (after smoothing and lifting) approximated uniformly over this bounded subset by trigonometric $\mathbb{C}^N$-valued polynomials $Q(x,y)$ with components $Q_r(x,y)$:

$$Q_r(x,y)=\sum_{i=0}^{k} a_{r,\lambda_i,\mu_i} e^{i(\lambda_i x+\mu_i y)}. \tag{3.1}$$

The vector space of such $\mathbb{C}^N$-valued polynomials, for a fixed finite number of distinct values of λ_i,μ_i, i.e., $\omega=(\lambda_i,\mu_i)\in K$, a fixed finite subset of $\mathbb{R}^2$, is denoted by $SE(2,N,K)$.

A trivial computation shows that semi-discrete hypoelliptic equation (2.8) restricts to $SE(2,N,K)$. It becomes

$$\frac{da_r^i}{dt}=-\frac{1}{2}\Big(\lambda_i\cos(\theta_r)+\mu_i\sin(\theta_r)\Big)^2 a_r^i+\frac{\beta}{2}\Big(a_{r+1}^i-2a_r^i+a_{r-1}^i\Big), \tag{3.2}$$

or, equivalently,

$$\frac{dA^i}{dt}=-\frac{1}{2}\mathrm{diag}_k\big(\lambda_i\cos(\theta_k)+\mu_i\sin(\theta_k)\big)^2 A^i+\Lambda_N A^i, \tag{3.3}$$

where A^i is the vector $(a_1^i,\dots,a_N^i)$ and the matrix Λ_N is the infinitesimal generator of the jump process with parameter β. The system of differential equations (3.2) is equipped with the initial condition $a_r^i(0)=a_{r,\lambda_i,\mu_i}$ with a_{r,λ_i,μ_i} from (3.1).

The following theorem holds.

Theorem 1. *For any almost periodic polynomial initial condition in $SE(2,N,K)$, the integration of the diffusion equation reduces to solving a finite set of independent linear ordinary differential equations of dimension N. Any continuous initial condition over a compact subset of $SE(2,N)$ can be uniformly approximated by such a polynomial.*

Differential equations (3.2) over $\mathbb{C}^N$ are not hard to tract numerically. They have an elliptic right hand term, and the Crank-Nicolson method (discussed in the next section) is recommended.

In fact, $SE(2,N,K)$ is the space of a unitary representation of $SE(2,N)$ which is not irreducible but splits into the direct sum of irreducible representations:

$$SE(2,N,K)=\bigoplus_{\omega\in K} SE(2,N,\{\omega\}).$$

This fact suggests that we can use our knowledge of the dual $\widehat{SE(2,N)}$ to reduce the computations. Actually, it is easy to check that for $\widetilde{\omega},\omega\in K$ such that $\widetilde{\omega}=R_r\omega$, if we call $\widetilde{A}$ and A the corresponding solutions of Equation (3.3) in $SE(2,N,\{\widetilde{\omega}\})$

and $SE(2,N,\{\omega\})$, respectively, we get:

$$\frac{dA}{dt} = -\frac{1}{2}\mathrm{diag}_k\big(\lambda_i\cos(\theta_k)+\mu_i\sin(\theta_k)\big)^2 A + \Lambda_N A,$$
$$\frac{dS^r\widetilde{A}}{dt} = -\frac{1}{2}\mathrm{diag}_k\big(\lambda_i\cos(\theta_k)+\mu_i\sin(\theta_k)\big)^2 S^r\widetilde{A} + \Lambda_N S^r\widetilde{A}.$$

So that it is not necessary to compute all the resolvents relative to each unitary irreducible representation. It is enough to do it for those corresponding to $\omega \in \widehat{SE(2,N)}$ only.

Theorem 2. *In theorem 1, if some points of K can be deduced one from the other by elementary rotations R_r then it is enough to compute the resolvents corresponding to a single among these points.*

This method could be very efficient in a general setting. The last considerations show that it is of numerical interest to put in K as much as possible points in the same orbits under the elementary rotations.

In our vision problem, the initial conditions are certainly very far from being almost periodic. Hence we preferred a more direct method, which is however closely related with this one. This is explained in the next section.

4. Final algorithm

In fact, images being given under the guise of a square table of real values (the grey levels), we have chosen to deal with periodic images over a basic rectangle, and to discretize with respect to the naturally discrete (x,y) variables. We take a mesh of $M_x \times M_y$ points on the (x,y)-plane, and the number of angles is N.

Remark 4. *In practice, in all the results we show, $M_x = M_y = M = 256$, and the number of angles $N \approx 30$.* ***We don't see any significant improvement for larger*** *N.*

Therefore, a function $\psi(x,y,\theta)$ over $SE(2,N)$ is approximated by a $M^2 \times N$ table $(\psi^p_{k,l})$, $p = 1,\dots,N$, $k,l = 1,\dots,M$. Hence, without loss of generality, we set for the discretization steps $\Delta x = \Delta y = \sqrt{M}$ and the mesh points are $x_k = \frac{k-1}{\sqrt{M}}$, $y_l = \frac{l-1}{\sqrt{M}}$. In this section, due to the periodicity, the upper index takes natural values modulo N and the lower indices take natural values modulo M.

Remind that the semi-discrete diffusion equation over $SE(2,N)$ is (2.8). For numerical solution of this equation we replace the differential operators $\frac{\partial}{\partial x}, \frac{\partial}{\partial y}$ by the discrete operators D_x, D_y, which act on $\mathbb{C}^{M^2}$:

$$D_x(\psi^p_{k,l}) = \frac{\psi^p_{k+1,l} - \psi^p_{k-1,l}}{x_{k+1} - x_{k-1}} = \frac{\sqrt{M}}{2}\big(\psi^p_{k+1,l} - \psi^p_{k-1,l}\big),$$
$$D_y(\psi^p_{k,l}) = \frac{\psi^p_{k,l+1} - \psi^p_{k,l-1}}{y_{l+1} - y_{l-1}} = \frac{\sqrt{M}}{2}\big(\psi^p_{k,l+1} - \psi^p_{k,l-1}\big).$$

Then we get the diffusion equation with totally discretized (i.e., with discretized space and angle variables) operator D, which acts on $\mathbb{C}^N \otimes \mathbb{C}^{M^2} \simeq \mathbb{C}^{N\cdot M^2}$:

$$\frac{d\psi^p_{k,l}}{dt} = \frac{1}{2} D(\psi^p_{k,l}), \quad \text{where} \tag{4.1}$$
$$D(\psi^p_{k,l}) = \big(\cos(e_p)D_x + \sin(e_p)D_y\big)^2(\psi^p_{k,l}) + \beta(\psi^{p-1}_{k,l} - 2\psi^p_{k,l} + \psi^{p+1}_{k,l}).$$

The initial condition for (4.1) is the discrete analog of the function $\overline{f}(x, y, \theta)$ obtained after the lift of the original image $f(x, y)$.

Remark 5. *For $M = 256$, $N = 30$ (4.1) is a fully coupled linear differential equation in $\mathbb{R}^K$, $K = 1,996,080$. Applying an implicit or semi-implicit finite difference scheme, one need to solve a system of $K^2 \approx 3.6 \times 10^{12}$ linear algebraic equations.*

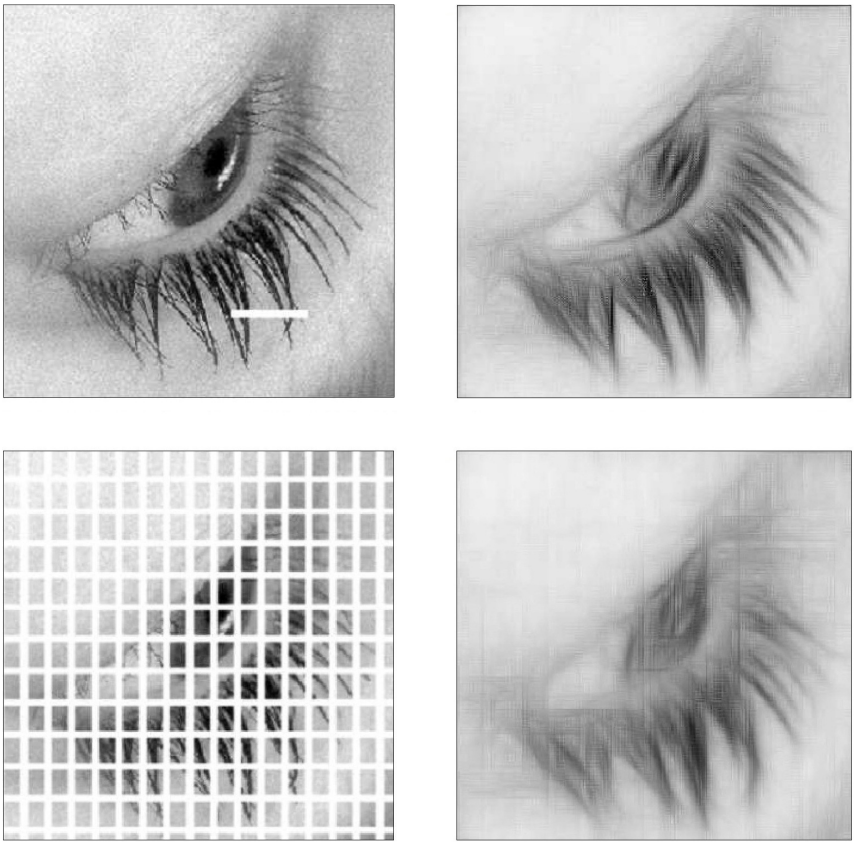

FIGURE 3. The initial corrupted images (left) and the images reconstructed via the hypoelliptic diffusion (2.13) with $\alpha = 0.25$ and time $T = 0.15$ (right, up), $T = 0.45$ (right, down).

As previously, it is natural to apply the Fourier transform over the abelian group $(\mathbb{Z}/M\mathbb{Z})^2$, which can be computed **exactly** by the standard FFT (Fast Fourier

Transform) algorithm. Let us denote by $\widehat{\psi}$ the Fourier transform of ψ:

$$\widehat{\psi}^p_{k,l} = \frac{1}{M}\sum_{r,s=1}^{M} \psi^p_{r,s} \exp\left(-2\pi i\left(\frac{(k-1)(r-1)}{M} + \frac{(l-1)(s-1)}{M}\right)\right).$$

A straightforward computation shows that

$$\widehat{D_x(\psi^p_{k,l})} = i\sqrt{M}\sin\left(2\pi\frac{k-1}{M}\right)\widehat{\psi}^p_{k,l}, \quad \widehat{D_y(\psi^p_{k,l})} = i\sqrt{M}\sin\left(2\pi\frac{l-1}{M}\right)\widehat{\psi}^p_{k,l},$$

and the Fourier transform maps the operator $\cos(e_p)D_x + \sin(e_p)D_y$ to the multiplication operator $\widehat{\psi}^p_{k,l} \to i\sqrt{M}\, a^p_{k,l}\widehat{\psi}^p_{k,l}$, where

$$a^p_{k,l} = \cos(e_p)\sin\left(2\pi\frac{k-1}{M}\right) + \sin(e_p)\sin\left(2\pi\frac{l-1}{M}\right).$$

Hence, the diffusion equation (4.1) is mapped to the following completely decoupled system of M^2 linear differential equations over $\mathbb{C}^N$:

$$\frac{d\widehat{\psi}_{k,l}}{dt} = A_{k,l}\,\widehat{\psi}_{k,l}, \quad \widehat{\psi}_{k,l} = (\widehat{\psi}^1_{k,l}, \ldots, \widehat{\psi}^N_{k,l}), \tag{4.2}$$

where $A_{k,l} = \frac{1}{2}\big(\Lambda_N - M\mathrm{diag}_p(a^p_{k,l})^2\big)$, and Λ_N is an almost tridiagonal $N \times N$ matrix: due to periodicity in p, Λ_N contains two extra non-zero elements in the right-up and left-low corners.

Therefore the solution of (4.2) is

$$\widehat{\psi}_{k,l}(t) = e^{tA_{k,l}}\widehat{\psi}_{k,l}(0), \tag{4.3}$$

where the initial function $\widehat{\psi}_{k,l}(0)$ is known. Finally, the solution of (4.1) is the inverse Fourier transform over $(\mathbb{Z}/M\mathbb{Z})^2$ of $\widehat{\psi}^p_{k,l}(t)$, obtained using the inverse FFT.

Theorem 3. *The solution of Equation* (4.1) *can be computed* ***exactly*** *by solving in parallel M^2 linear differential equations in dimension N.*

For instance, for $M = 256$ and $N = 30$, this is solving 65536 linear differential equations in dimension 30.

Remark 6. *1. The complexity of the FFT used twice in our algorithm (including the inverse transform) is negligible in front of the complexity of the numerical integration of the decoupled linear differential equations.*

2. The discretized diffusion (4.1) *can be numerically integrated with the semi-explicit Crank-Nicolson scheme. The convergence of this scheme for the considered class of equations and some estimations are well known; see e.g.* [29, chapter 5]. *Note that the matrices $A_{k,l}$ are tridiagonal plus two terms in the right-up and left-low corners (coming from Λ_N due to periodicity). An effective algorithm for solving such linear system is suggested in* [1].

3. Formula (4.3) *for solutions of the linear differential equations* (4.2) *has an obvious advantage. Once M, N and α (or, equivalently, β) are fixed, the matrices $A_{k,l}$* ***are universal****, and therefore their exponentials can be computed once for all. Moreover, using a time step τ and the formula $e^{n\tau A_{k,l}} = \big(e^{\tau A_{k,l}}\big)^n$, it is enough to compute only the exponential $e^{\tau A_{k,l}}$.*

4. In fact, it is not necessary to compute M^2 exponentials of matrices: it is enough to compute them at the points k, l that fall in the dual space $\widehat{SE(2,N)}$.

This is much less. For large N, is number is of order M in place of M^2. Here, the structure of $SE(2,N)$ is crucial, and specially formula (2.10).

5. Heuristic complements

It has to be noticed that:

- The treatment of images up to now is essentially global.
- It is not necessary to know where the image is corrupted.

Presumably, the visual cortex V1 is also able in some cases to detect that the image is corrupted at some place, and to take this a-priori knowledge into account.

We tried to investigate methods that would improve on our algorithm in this direction. These methods are based upon the general idea of distinguishing between "good" and "bad" points (pixels) of the image under reconstruction. We would like to preserve good points from the diffusion or at least to weaken the effect of the the diffusion at these points, while on the set of bad points the diffusion should proceed normally. In this section, we present two heuristic methods:

- Static restoration method, where the sets of good and bad points do not change along the treatment.
- Dynamic restoration method, where some bad points may become good, and then the sets of good and bad points change along the treatment.

5.1. **Restoration: downstairs or upstairs?** One natural idea would be to iterate the following steps:

- Lift the plane image to $PT\mathbb{R}^2$.
- Integrate the diffusion equation for some fixed small τ.
- Project the solution down to the plane.
- Restore the non-corrupted part of the initial image.

In practice, this idea does not work at all. The main reason is that the diffusion acts on both the corrupted and the non-corrupted parts, and there is not good coincidence at the frontier after the restoration.

All variations of the previous idea, at the level of the plane image do not provide acceptable results. From what we conclude that it is necessary to proceed the restoration of the the non-corrupted part at the level of the lifted image, i.e., on the bundle $PT\mathbb{R}^2$.

5.2. **Static restoration (SR).** Assume that points (x,y) of the image are separated into the set G of good (non-corrupted) and the set B of bad (corrupted) points, $f(x,y)=0$ for all $(x,y)\in B$ and $f(x,y)>0$ for all $(x,y)\in G$. The idea of the restoration procedure is to "mix" the solution $\psi(x,y,\theta,t)$ of the diffusion equation with the initial function $\psi(x,y,\theta,0)=\overline{f}(x,y,\theta)$ at each point $(x,y)\in G$.

The "mixing" is fulfilled many times during the integration of our equation. Namely, split the segment $[0,T]$ into n small intervals with the mesh points $t_i=i\tau$, $\tau=T/n$, $i=0,1,\dots,n$, and proceed the integration of our equation on each $[t_i,t_{i+1}]$ with the initial condition

$$\psi\big|_{t=t_i}=\begin{cases}\psi(x,y,\theta,t_i), & \text{if } (x,y)\in B,\\ \sigma(x,y,t_i)\,\psi(x,y,\theta,t_i), & \text{if } (x,y)\in G,\end{cases}$$

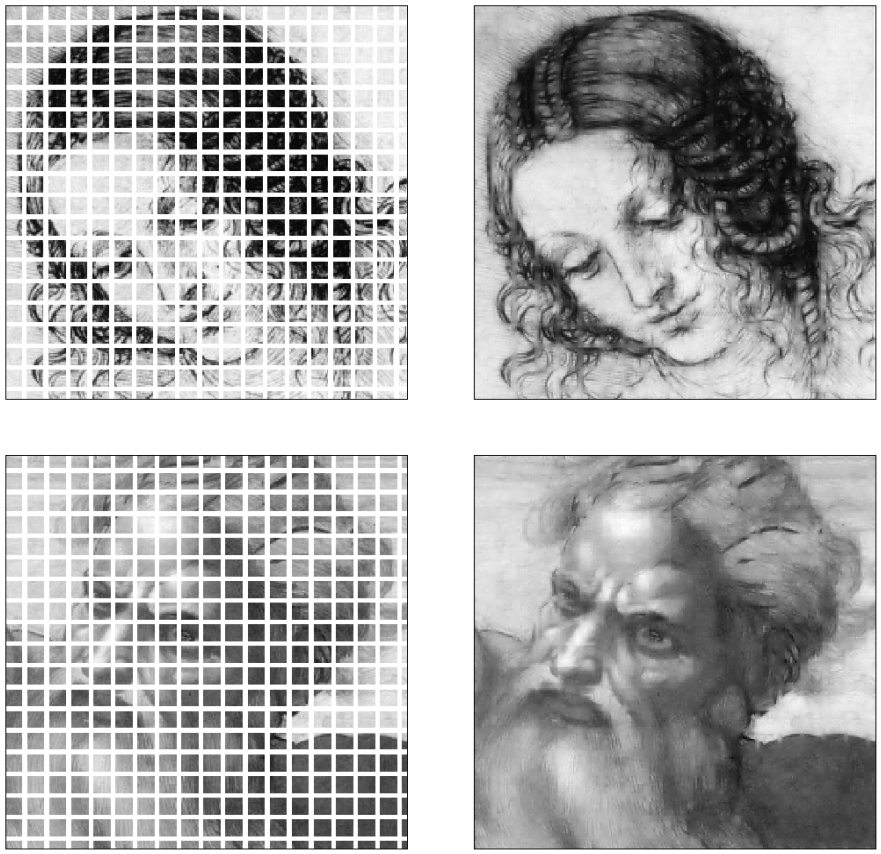

FIGURE 4. The initial corrupted images (left) and the images reconstructed via the hypoelliptic diffusion (2.13) and the SR procedure with parameters from Table 1 (right).

where the function $\psi(x, y, \theta, t_i)$ is computed after integration on the previous interval, and the factor $\sigma(x, y, t_i)$ is defined by

$$\sigma(x, y, t_i) = \frac{\epsilon h(x, y, 0) + (1 - \epsilon)h(x, y, t_i)}{h(x, y, t_i)}, \qquad h(x, y, t) = \max_{\theta} \psi(x, y, \theta, t),$$

$0 \leq \epsilon \leq 1$. After that we obtain the function $\psi(x, y, \theta, t_{i+1})$ and repeat the procedure on the next interval.

This procedure essentially depends on two parameters that can be chosen experimentally: the natural number n (number of treatments) and the coefficient ϵ, which defines the strength of each treatment.

5.3. **Dynamic restoration (DR).** There is a defect in the procedure described above: different corrupted parts of the image have different velocities of reconstruction. This effect can cause serious defects.

For instance, consider two different points (x', y') and (x'', y'') of the set B. Let T' be the time of the diffusion required for (x', y') being reconstructed well, T'' be the same for (x'', y''), and $T' \ll T''$. Applying the diffusion with $T \approx T'$, we get

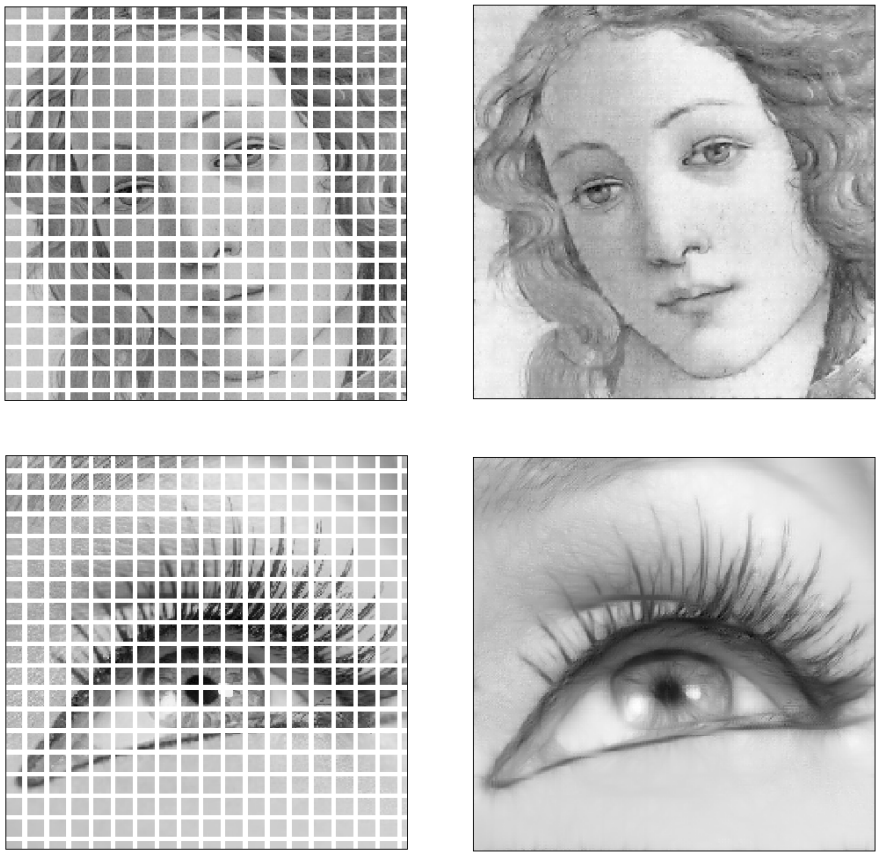

FIGURE 5. The initial corrupted images (left) and the images reconstructed via the hypoelliptic diffusion (2.13) and the DR procedure with parameters from Table 1 (right).

the image not reconstructed enough at (x'', y''). On the other hand, in the case $T \approx T''$ the image is reconstructed well at (x'', y''), but a defect near the point (x', y') can appear. This brings us to a natural idea: to use the diffusion with the time T depending on a point (x, y). A simple way to realize it is to make the sets of good and bad points changing in time so that a bad point at some moment may become good, and the effect of the diffusion at this point is not essential anymore.

Define the initial set of good points G_0 as before (the set of non-corrupted points of the image) and define G_i, $i = 1, \dots, n$, as follows:

Denote by $f_{i-1}(x, y)$ the image at step $i - 1$. Then G_i contains G_{i-1} and all points (x, y) of the boundary ∂B_{i-1} such that the value $f_{i-1}(x, y)$ is larger than the average value of f_{i-1} over the points of B_{i-1} in the 9-points neighborhood of (x, y). The set B_i is defined as the complement of G_i.

Appendix A. Results with high corruption rates

Here we present a series of results of reconstruction with high corruption rates via the hypoelliptic diffusion (2.13) and the DR procedure with different parameters found experimentally and listed in Table 1 below.

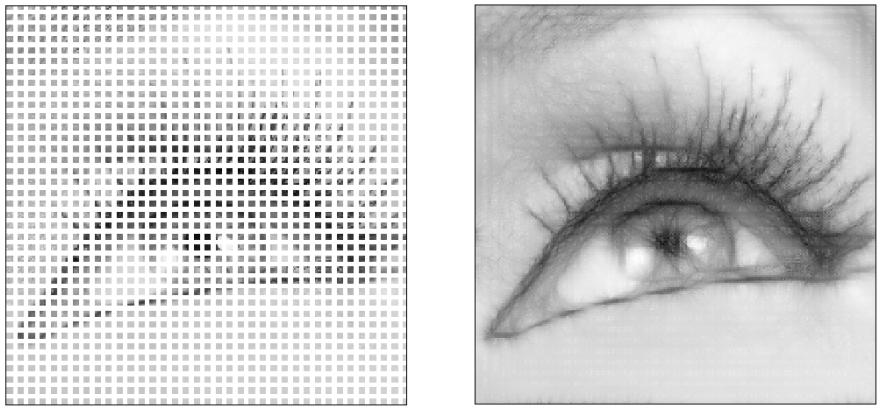

Figure 6.

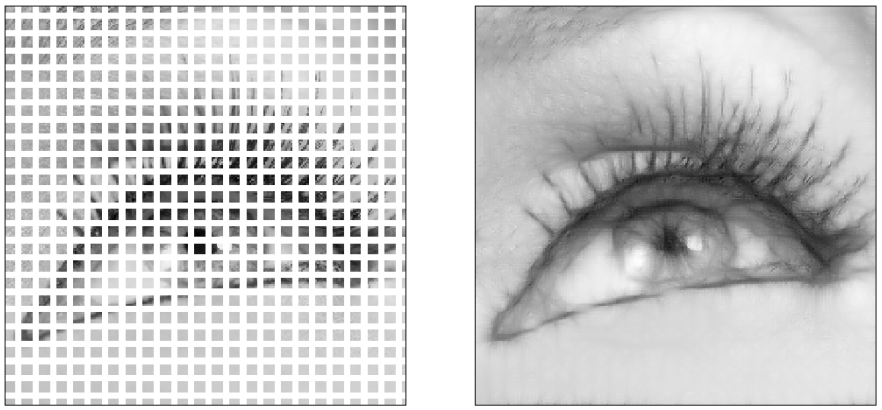

Figure 7.

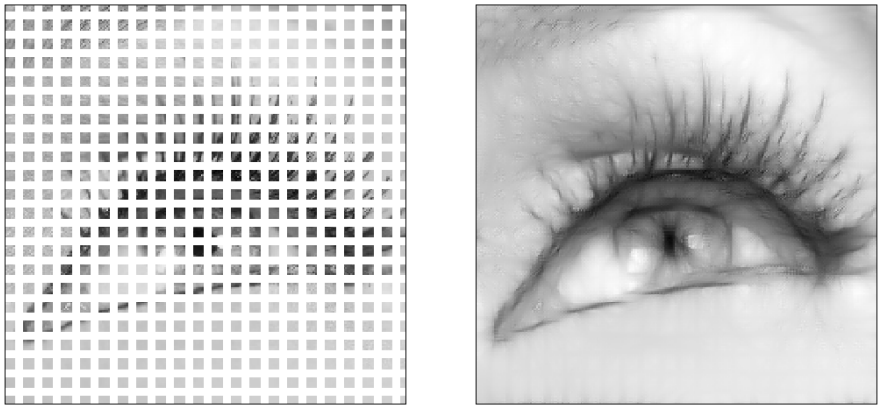

FIGURE 8.

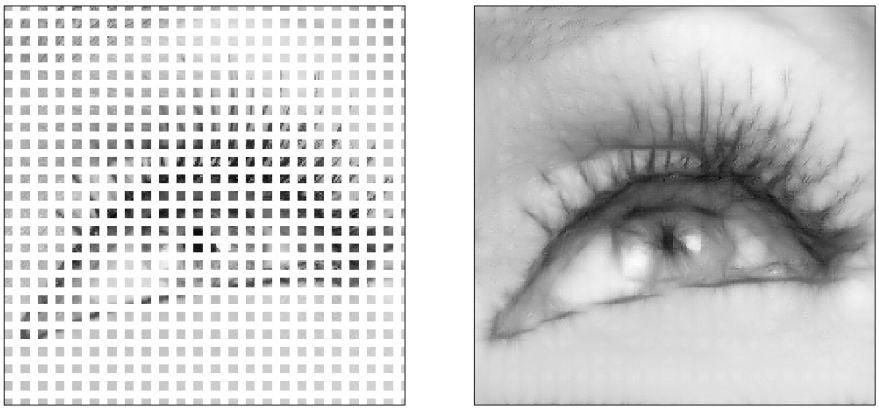

FIGURE 9.

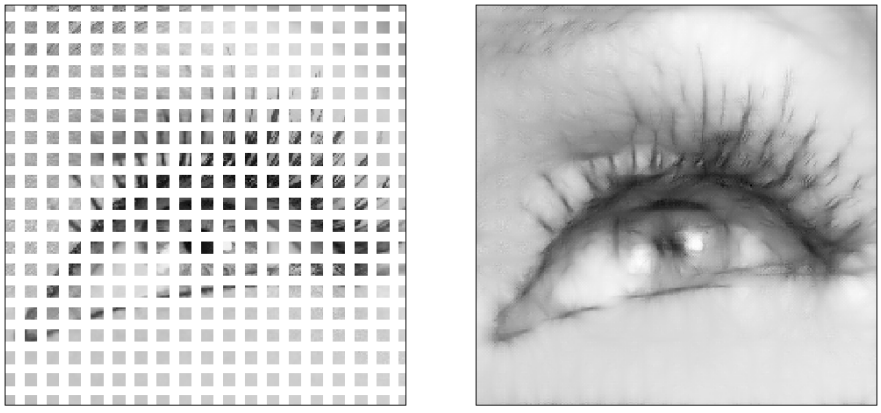

FIGURE 10.

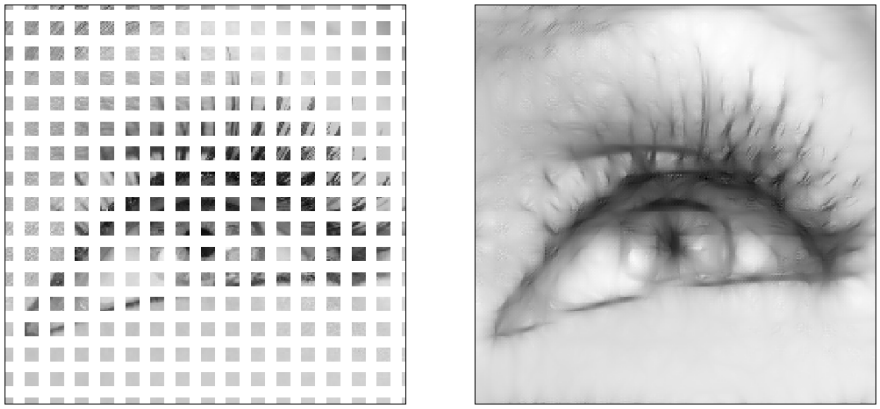

FIGURE 11.

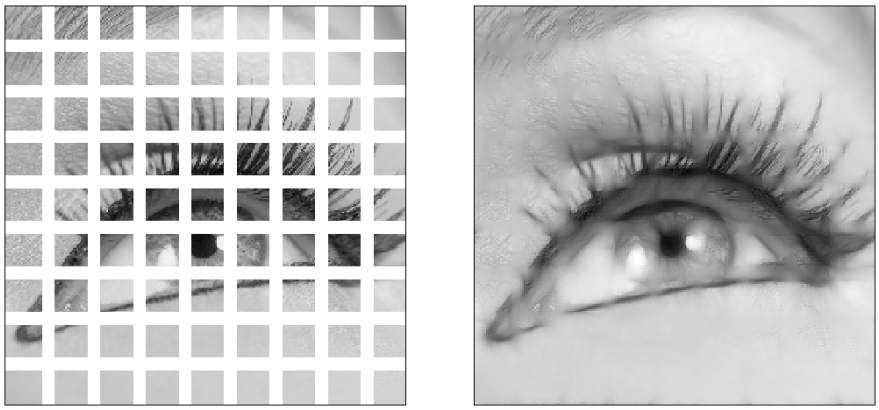

FIGURE 12.

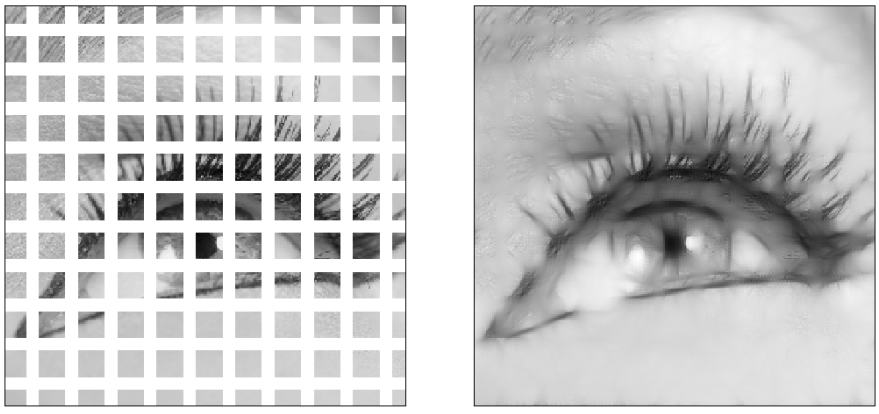

FIGURE 13.

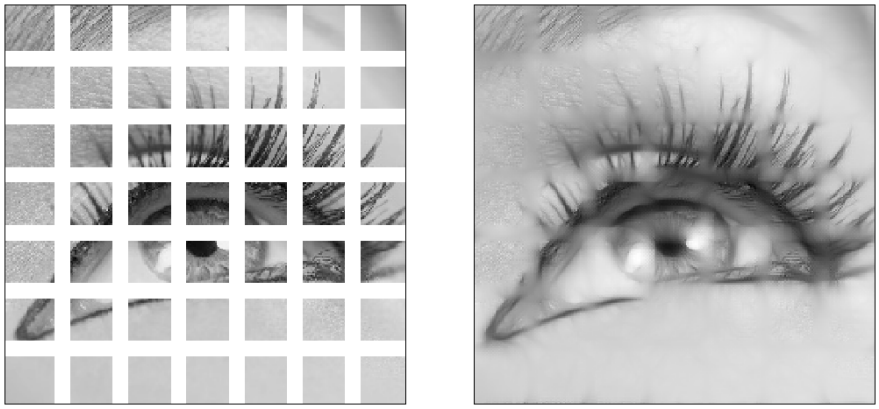

FIGURE 14.

TABLE 1. Parameters of the reconstruction for Fig. 4 – 14. The images have resolution 256×256 (pixels) and the corrupted parts consist of vertical and horizontal lines of width w:

Figure:	Diffusion:		Restoration:		Corruption:	
	α	T	n	ϵ	w, pixels	Total, %
4, up	2.0	0.8	200	0.5	3	37
4, down	3.0	0.2	200	0.5	3	37
5, up	4.0	0.2	200	0.5	3	37
5, down	0.30	4.0	160	0.5	3	37
6	0.30	4.0	160	0.5	3	67
7	0.30	4.0	160	0.5	4	58
8	0.30	4.0	160	0.5	5	65
9	0.40	4.0	120	0.5	5	69
10	0.35	5.0	160	0.5	6	67
11	0.33	6.0	180	0.5	7	68
12	0.33	6.0	250	0.5	8	43
13	0.33	6.0	250	0.5	8	53
14	0.33	6.0	250	0.5	10	41

APPENDIX B. THEORETICAL COMPLEMENTS

In this appendix, we collect shortly a few results needed for the understanding of the paper.

B.1. **The Generalized Fourier Transform (GFT).** Given a locally compact unimodular topological group G of Type I[9], the dual $\widehat{G}$ is the set of (strongly) continuous complex unitary irreducible representations $(\chi_{\widehat{g}}, H_{\widehat{g}})$ of G. For $\widehat{g} \in \widehat{G}$, $\chi_{\widehat{g}} \colon G \to U(H_{\widehat{g}})$, the unitary group of the complex Hilbert space $H_{\widehat{g}}$. The space of complex L^2 functions over G with respect to the Haar measure is denoted by

[9]We do not say what type I means. We just need here to know that both $SE(2)$ and $SE(2,N)$ are type I. For instance, any connected semi-simple or nilpotent group is type I.

$L^2(g, dg)$. The generalized Fourier transform (GFT) of $f \in L^2(g, dg)$ is defined by[10]:

$$\widehat{f}(\widehat{g}) = \int_G f(g)\chi_{\widehat{g}}(g^{-1})\, dg. \tag{B.1}$$

The operator $\widehat{f}(\widehat{g})$ is Hilbert-Schmidt over $H_{\widehat{g}}$ and there is a measure $d\widehat{g}$ over $\widehat{G}$, called the Plancherel measure, such that the GFT is an isometry to $L^2(\widehat{g}, d\widehat{g})$, where the space $L^2(\widehat{g}, d\widehat{g})$ is the continuous Hilbert sum of the spaces of Hilbert-Schmidt operators over the spaces $H_{\widehat{g}}$, with respect to Plancherel's measure. As a consequence, we have the inversion formula:

$$f(g) = \int_{\widehat{G}} \widehat{f}(\widehat{g})\chi_{\widehat{g}}(g)\, d\widehat{g}. \tag{B.2}$$

The GFT is a natural extension of the ordinary Fourier transform over abelian groups and it has all the corresponding properties, such as: mapping convolution to product, etc. (see [3]).

As in the case of the usual heat equation over $\mathbb{R}^n$, we use it to solve our heat equations over the groups $SE(2)$ and $SE(2, N)$.

B.2. **Bohr Compactification and Almost Periodic Functions.** The Bohr compactification of a topological group G is the universal object $(G^\flat, \widetilde{\sigma})$ in the category of diagrams:

$$\sigma\colon G \to H,$$

where σ is a continuous homomorphism from G to a compact group H. If the mapping $\widetilde{\sigma}\colon G \to G^\flat$ is injective, G is called maximally almost periodic (MAP).

The set $AP(G)$ of almost periodic functions over G is the pull back by $\widetilde{\sigma}$ of the set of continuous functions over $G^\flat$.

The group G is MAP iff the continuous unitary finite dimensional representations of G separate the points. A connected locally compact group is MAP iff it is the direct product of a compact group by $\mathbb{R}^n$. The group $SE(2, N)$ is MAP, while $SE(2)$ is not.

A continuous function $f \in AP(G)$ iff its right (or left) translated form a relatively compact subset of $E(G)$, the set of bounded continuous functions over G, iff it is a uniform limit of coefficients of unitary irreducible representations of G. If G is MAP, $AP(G)$ is dense in the space of continuous functions over G, in the topology of uniform convergence over compact sets.

For duality over MAP groups, see [11] and the book [23]. For introduction to almost periodic functions, see the original paper [42] and the nice exposition [19].

B.3. **Proof that expressions (2.10) and (2.12) are identical.** In this section, all integer indices take values between 1 and N, and addition is always modulo N.

[10]As usual, the integral below is well defined for $f \in L^1(G, dg)$ only, but is extended by continuity.

Set $M_{\lambda,\nu}(t) = e^{\widetilde{A}_{\lambda,\nu}t}$, where the matrix $\widetilde{A}_{\lambda,\nu}$ is defined in (2.9). Then we need to establish the identity of the two expressions:

$$D^1_t(z,e_r) = \int\limits_{\widehat{SE(2,N)}} \operatorname{trace}\Big(M_{\lambda,\nu}(t)\cdot \operatorname{diag}_k\Big(e^{i\langle V_{\lambda,\nu},R_k z\rangle}\Big)S^r\Big)\lambda d\lambda d\nu,$$

$$D^2_t(z,e_r) = \int\limits_{\mathbb{R}^2} \big(M_{\lambda,\nu}(t)\delta_N\big)_r\, e^{i\langle V_{\lambda,\nu},z\rangle}\lambda d\lambda d\nu.$$

Set

$$M^r_{\lambda,\nu}(t) = e^{\widetilde{A}^r_{\lambda,\nu}t}, \quad \widetilde{A}^r_{\lambda,\nu} = \Lambda_N - \operatorname{diag}_k\big(\lambda^2\cos^2(e_{k+r}-\nu)\big).$$

The following fact is crucial:

$$S^{-r}M_{\lambda,\nu}(t)S^r = M^r_{\lambda,\nu}(t), \tag{B.3}$$

where S is the shift matrix over $\mathbb{C}^N$ (i.e., $Se_k = e_{k+1}$ for $k = 1,\dots,N-1$, and $Se_N = e_1$). The equality (B.3) follows from $S^{-r}\widetilde{A}^r_{\lambda,\nu}S^r = \widetilde{A}_{\lambda,\nu}$, a consequence of $S^{-r}\Lambda_N S^r = \Lambda_N$ and of the general relation

$$(S^{-r}BS^r)_{n,m} = B_{n-r,m-r}, \tag{B.4}$$

which holds true for any $N\times N$ matrix B.

An immediate computation shows that

$$D^1_t(z,e_r) = \int\limits_{\widehat{SE(2,N)}} \sum_n \Big(M_{\lambda,\nu}(t)\cdot \operatorname{diag}_k\Big(e^{i\langle V_{\lambda,\nu},R_k z\rangle}\Big)\Big)_{n+r,n}\lambda d\lambda d\nu = \tag{B.5}$$

$$\int\limits_{\widehat{SE(2,N)}} \sum_n \big(M_{\lambda,\nu}(t)\big)_{n+r,n} e^{i\langle V_{\lambda,\nu},R_n z\rangle}\lambda d\lambda d\nu.$$

On the other hand, using the relations (B.3) and (B.4), we have:

$$D^2_t(z,e_r) = \int\limits_{\mathbb{R}^2} \big(M_{\lambda,\nu}(t)\delta_N\big)_r\, e^{i\langle V_{\lambda,\nu},z\rangle}\lambda d\lambda d\nu = \int\limits_{\mathbb{R}^2} \big(M_{\lambda,\nu}(t)\big)_{r,N}\, e^{i\langle V_{\lambda,\nu},z\rangle}\lambda d\lambda d\nu =$$

$$\int\limits_{\widehat{SE(2,N)}} \sum_n \big(M^n_{\lambda,\nu}(t)\big)_{r,N}\, e^{i\langle V_{\lambda,\nu-e_n},z\rangle}\lambda d\lambda d\nu =$$

$$\int\limits_{\widehat{SE(2,N)}} \sum_n \big(S^{-n}M_{\lambda,\nu}(t)S^n\big)_{r,N}\, e^{i\langle V_{\lambda,\nu},R_{-n}z\rangle}\lambda d\lambda d\nu =$$

$$\int\limits_{\widehat{SE(2,N)}} \sum_n \big(M_{\lambda,\nu}(t)\big)_{r-n,N-n}\, e^{i\langle V_{\lambda,\nu},R_{-n}z\rangle}\lambda d\lambda d\nu.$$

Finally, changing n for $-n$ and observing that $N+n = n$, we get the following expression:

$$D^2_t(z,e_r) = \int\limits_{\widehat{SE(2,N)}} \sum_n \big(M_{\lambda,\nu}(t)\big)_{n+r,n}\, e^{i\langle V_{\lambda,\nu},R_n z\rangle}\lambda d\lambda d\nu,$$

which is exactly (B.5).

Acknowledgement 1. *The authors thank Jean Petitot for his valuable comments and suggestions, and Prof. Eric Busvelle for his help.*

Acknowledgement 2. *This research has been supported by the Europen Research Council, ERC StG 2009 "GeCo Methods" (contract 239748), by the ANR "GCM" (programme blanc NT09-504490), and by the DIGITEO project CONGEO.*

References

[1] A.A. Abramov, V.B. Andreev, On the application of the method of successive substitution to the determination of periodic solutions of differential and differences equations, Zh. Vychisl. Mat. Mat. Fiz., 3.2, 1963, pp. 377–381.

[2] A. Agrachev, D. Barilari, Sub-Riemannian structures on 3D Lie groups, J. Dynamical and Control Systems (2012), v.18, 21-44.

[3] A. Agrachev, U. Boscain, J.-P. Gauthier, F. Rossi, The intrinsic hypoelliptic Laplacian and its heat kernel on unimodular Lie groups, J. Funct. Anal., 256 (2009), pp. 2621–2655.

[4] A.A. Agrachev, Yu. L. Sachkov, Control Theory from the Geometric Viewpoint, Encyclopedia of Mathematical Sciences, v. 87, Springer, 2004.

[5] N.U. Ahmed, T.E. Dabbous, Nonlinear Filtering of systems governed by ITO Differential Equations with Jump Parameters, Journal of Mathematical Analysis and Applications, 115 (1986), pp. 76–92.

[6] A.Ardentov, A.Mashtakov, Y. Sachkov, Inpainting via sub-Riemannian minimizers on the group of rototranslations, Numer. Math. Theor. Meth. Appl., Vol. 6, No. 1, pp. 95-115.

[7] U. Boscain, G. Charlot, F. Rossi, Existence of planar curves minimizing length and curvature, Proceedings of the Steklov Institute of Mathematics, vol. 270, n. 1, pp. 43-56, 2010.

[8] U. Boscain, J. Duplaix, J.P. Gauthier, F. Rossi, Anthropomorphic image reconstruction via hypoelliptic diffusion. SIAM J. CONTROL OPTIM., Vol. 50, no. 3 (2012), pp. 1309–1336.

[9] U. Boscain, R. Duits, F. Rossi, Y. Sachkov, Curve cuspless reconstruction via sub-Riemannian geometry. arXiv:1203.3089.

[10] F. Cao, Y. Gousseau, S. Masnou, P. Pérez, Geometrically guided exemplar-based inpainting, submitted.

[11] H. Chu, Compactification and duality of topological groups, Trans. Am. Math. Soc. 123, 1966, pp. 310–324.

[12] G.S. Chirikjian, A.B. Kyatkin, Engineering applications of noncommutative harmonic analysis, CRC Press, Boca Raton, FL, 2001.

[13] G. Citti, A. Sarti, A cortical based model of perceptual completion in the roto-translation space, J. Math. Imaging Vision 24 (2006), no. 3, pp. 307–326.

[14] C. Corduneanu, N. Gheorgiu, V. Barbu, Almost Periodic Functions, second edition,Chelsea Publishing Company, 1989.

[15] J. Damon, Generic structure of two-dimensional images under Gaussian blurring, SIAM J. Appl. Math., Vol. 59, No. 1 (1998), pp. 97–138.

[16] R. Duits, M. van Almsick, The explicit solutions of linear left-invariant second order stochastic evolution equations on the 2D Euclidean motion group. Quart. Appl. Math. 66 (2008), pp. 27–67.

[17] R. Duits, E.M. Franken, Left-invariant parabolic evolutions on SE(2) and contour enhancement via invertible orientation scores, Part I: Linear Left-Invariant Diffusion Equations on $SE(2)$ Quart. Appl. Math., 68 (2010), pp. 293–331.

[18] R. Duits, E.M. Franken, Left-invariant parabolic evolutions on SE(2) and contour enhancement via invertible orientation scores, Part II: nonlinear left-invariant diffusions on invertible orientation scores Quart. Appl. Math., 68 (2010), pp. 255–292.

[19] J. Dixmier, Les C^*-algèbres et leurs représentations, second edition, Gauthier-Villars, Paris, 1969.

[20] E.M. Franken, Enhancement of Crossing Elongated Structures in Images. Ph. D. Thesis, Eindhoven University of Technology, 2008, Eindhoven, http://alexandria.tue.nl/extra2/200910002.pdf

[21] E.M. Franken, R. Duits, Crossing-Preserving Coherence-Enhancing Diffusion on Invertible Orientation Scores., IJCV, 85 (3), 2009, pp. 253–278.

[22] M. Gromov, Carnot-Caratheodory spaces seen from within, in Sub-Riemannian geometry, Progr. Math., vol. 144, Birkhäuser, Basel, 1996, pp. 79–323.
[23] H. Heyer, Dualität über Lokal Kompakter Gruppen, Springer Berlin, 1970.
[24] R.K. Hladky, S.D. Pauls, Minimal Surfaces in the Roto-Translation Group with Applications to a Neuro-Biological Image Completion Model, J. Math. Imaging Vis. 36 (2010), pp. 1–27.
[25] W. C. Hoffman, The visual cortex is a contact bundle, Appl. Math. Comput., 32, pp.137–167, 1989.
[26] L. Hörmander, Hypoelliptic Second Order Differential Equations, Acta Math., 119 (1967), pp. 147–171.
[27] D. H. Hubel, T. N. Wiesel, Receptive Fields Of Single Neurones In The Cat's Striate Cortex, Journal of Physiology, (1959) 148, 574-591.
[28] M. Langer, Computational Perception, Lecture Notes, Centre for Intelligent Machines, 2008, http://www.cim.mcgill.ca/˜langer/646.html
[29] G.I. Marchuk, Methods of Numerical Mathematics. Application of Mathematics, 2. Springer-Verlag, 1982.
[30] D. Marr, E. Hildreth, Theory of Edge Detection, Proceedings of the Royal Society of London. Series B, Biological Sciences, Vol. 207, No. 1167. (Feb. 29, 1980), pp. 187–217.
[31] I. Moiseev, Yu. L. Sachkov, Maxwell strata in sub-Riemannian problem on the group of motions of a plane, ESAIM: COCV 16, no. 2 (2010), pp. 380–399.
[32] D. Mumford, Elastica and computer vision. Algebraic Geometry and Its Applications. Springer-Verlag, 1994, pp. 491–506.
[33] L. Peichl, H. Wässle, Size, scatter and coverage of ganglion cell receptive eld centres in the cat retina, J. Physiol., Vol. 291, 1979, pp. 117–41.
[34] J. Petitot, Y. Tondut Vers une Neuro-geometrie. Fibrations corticales, structures de contact et contours subjectifs modaux, Mathématiques, Informatique et Sciences Humaines, EHESS, Paris, Vol. 145, pp. 5–101, 1998.
[35] J. Petitot, Vers une Neurogéométrie. Fibrations corticales, structures de contact et contours subjectifs modaux, Math. Inform. Sci. Humaines, no. 145 (1999), pp. 5–101.
[36] J. Petitot, Neurogéométrie de la vision – Modèles mathématiques et physiques des architectures fonctionnelles, Les Éditions de l'École Polythecnique, 2008.
[37] Yu. L. Sachkov, Conjugate and cut time in the sub-Riemannian problem on the group of motions of a plane, ESAIM: COCV 16 (2010), pp. 1018–1039.
[38] Yu. L. Sachkov, Cut locus and optimal synthesis in the sub-Riemannian problem on the group of motions of a plane, ESAIM: COCV 17 (2011), pp. 293–321.
[39] G. Sanguinetti, G. Citti, A. Sarti, Image completion using a diffusion driven mean curvature flowin a sub-Riemannian space, in: Int. Conf. on Computer Vision Theory and Applications (VISAPP'08), FUNCHAL, 2008, pp. 22–25.
[40] N.Y. Vilenkin, Special functions and the theory of group representations, American Mathematical Soc., 1968.
[41] G. Warner, Harmonic Analysis on Semi-Simple Groups, Vols. 1 and 2, Springer-Verlag, 1972.
[42] A. Weil, L'intégration dans les groupes topologiques et ses applications. Publications de L'institute de Mathématique de L'université de Strasbourg. Paris, Hermann, 1953.

CNRS, CMAP, École Polytechnique CNRS, Route de Saclay, 91128 Palaiseau Cedex, France; INRIA Team GECO
E-mail address: boscain@cmap.polytechnique.fr
URL: http://www.cmapx.polytechnique.fr/~boscain/

Centre for Wind Energy and Atmospheric Flows, Faculdade de Engenharia da Universidade do Porto, Rua Dr. Roberto Frias s/n, 4200-465 Porto, Portugal; International Institute of Earthquake Prediction Theory and Mathematical Geophysics, Profsoyuznaya str. 84/32, 117997 Moscow, Russia
E-mail address: roman@mitp.ru

LSIS, UMR CNRS 7296, Universté de Toulon USTV, 83957, La Garde Cedex, France; INRIA Team GECO
E-mail address: gauthier@univ-tln.fr
URL: http://www.lsis.org/jpg

CMAP, École Polytechnique CNRS, Route de Saclay, 91128 Palaiseau Cedex, France
E-mail address: alexey-remizov@yandex.ru